Supplemental Data

Supplemental Methods

Mice

All animals were maintained and experiments were performed in accordance with institutional guidelines at the University of California, San Diego. A BAC plasmid containing 83.2 kbp upstream and 87.4 kbp downstream of the *Cyclin A2* transcription start site was genetically engineered to insert a lacZ cassette flanked by loxP sites, followed by an EGFP cassette in-frame immediately before the stop codon of *Cyclin A2* (1). Thus, CyclinA2-βgalactosidase (βgal) would be expressed under control of *CyclinA2*. Numb flox/flox (2), NumbL flox/flox (3), Yap1 flox/flox (4) mice, TnT-Cre (5), Meox2-Cre (6), R26-mTmG (7), were purchased from JAX. ErbB2 null mice (8) and TNR Notch indicator (9) were kindly provided by Dr. KF Lee (The Salk Institute, La Jolla, USA) and Dr. T Reya (University of California, San Diego, La Jolla, USA) respectively. Numb null, NumbL null mutants were generated by crossing Numb f/f, NumbL f/f into Meox2-Cre. Numb cKO was generated by crossing TnT-Cre;Numb-Δ/wt with Numb-flox/flox mice, while Numb/NumbL cKO was generated by crossing TnT-Cre;Numb-Δ/wt;NumbL-Δ/Δ with Numb-flox/flox;NumbL-Δ/Δ mice.

Plasmid construction

pEF/V5 vectors (Life Technologies), modified by incorporation of a FLAG-tag and a Myc-tag, and an expression vector encoding the puromycin resistance gene, were kindly provided by Dr. T. Nakamura (Kansai Medical University, Hirakata, Japan). cDNAs of p72 and p66 isoforms of Numb were kindly provided by CJM. pX335 and pEGxxFP was purchased from Addgene. Mouse full-length cDNAs, Numb p65 (BC033459), NumbL (BC068116), ErbB2 (BC046811), ErbB4 (BC156355), Rab7b (NM145509), Yap1 (NM001171147) and Stat5 (NM011488) were purchased from Riken Bioresource

Center, Source BioScience, or Sino Biological Inc. Mouse full-length cDNAs of Rab5a, 7a, and 11a were cloned from first strand cDNA synthesized from total RNA extracted from embryonic mouse heart or lung tissue. The following cDNA fragments were amplified by inverse PCR, followed by PCR mediated recombination. 1) Numb ΔPTB (Δnucleotide (nt) 132-769), ΔNumbF (Δnt 1019-1270), ΔC1 (Δnt 1775-2068), ΔC2 (Δnt 1352-2068), 2) ErbB2 ΔPTK (Δnt 2388-3224), ΔC1 (Δnt 3273-3680), ΔC2 (Δnt 3681-4022), 3) Stat5a ΔN1 (Δnt 337-723), ΔN2 (Δnt 733-1323), ΔDBD (Δnt 1339-2049), ΔSH2 (Δnt 2050-2715), 4) Yap1 ΔN (Δnt 210-662), ΔWW (Δnt 669-980), ΔTA (Δnt 992-1673). Each cDNA sequence is numbered according to the GenBank™ accession number listed above. These fragments were subcloned into the modified pEF/V5 vector, and utilized for protein expression in mammalian cells. For the tagged ErbB2 construct stably expressed in HeLa cell lines, mCherry and HA coding sequences were inserted in-frame immediately before the stop codon of ErbB2 cDNA, then subcloned into the modified pEF/V5 vector. The endogenous signal sequence of ErbB2 was eliminated, substituting a preprotrypsin signal sequence-Flag-Venus cassette at the N-terminus of ErbB2, so that the tagged construct would be cleaved just before the Flag-tag. The preprotrypsin signal sequence-Flag-Venus cassette was kindly provided by Dr. T Nakamura (Kansai Medical University, Hirakata, Japan) (10).

Immunofluorescence

Mouse embryos and HeLa cells were fixed in 4% paraformaldehyde (PFA), then mouse embryos were embedded in Tissue-Tek OCT compound. Mouse frozen sections or HeLa cells were permeabilized with 0.1% Triton, and subsequently subjected to immunostaining. Primary antibodies used for immunohistochemistry were anti-Troponin T monoclonal (13-11, Thermo Scientific, 1:200), anti-GFP

polyclonal (ab290, Abcam, 1:200), anti-p57 Kip2 polyclonal (ab4058, Abcam, 1:50), anti-Flk1 polyclonal (AF644, R&D Systems, 1:50), anti-Numb monoclonal (C29G11, Cell Signaling, 1:200), anti-Yap1 monoclonal (2F12, Abnova, 1:60), anti-ErbB2 monoclonal (340554, Becton Dickinson, 1:20) or (3B1, Abnova, 1:100), anti-Lamp1 monoclonal (1D4B, DSHB, 1:50) or polyclonal (ab24170, Abnova, 1:100), anti-EEA1 polyclonal (1G11, Abcam, 1:100), anti-Flag M2 monoclonal (Sigma-Aldrich, 1:200). Secondary antibodies used were Alexa 488, 555, or 647 anti-rabbit, mouse, rat, or goat IgG (Life Technologies), with or without Alexa Fluor 568 or 647 phalloidin staining, followed by nuclear staining with DAPI. Stained sections/cells were mounted with Dako fluorescence mounting medium, and visualized using an Olympus confocal microscope (FV1000), Deltavision OMX microscope, or Zeiss LSM8 Airyscan. EdU (Life Technologies) was intraperitoneally injected two hours before embryo dissection, and detected with Click-iT EdU Alexa Fluor 647 Imaging Kit (Life Technologies).

Laser capture microdissection

Frozen tissue sections of ED10.5 mouse embryos were stained with Eosin. After dehydration, sections were subjected to laser capture microdissection with an MMI CellCut laser microdissection system. High magnification was used to delineate myocardial cells and avoid contamination with endocardial cells (Olympus UPLFLN 40xPH). Tissues were collected from two independent experiments.

Reverse transcription-polymerase chain reaction and quantitative PCR

Total RNAs were extracted using RNeasy Plus Mini Kit (QIAGEN), Absolutely RNA Nanoprep Kit (Agilent Technologies), or Picopure RNA isolation kit (Life Technologies), depending on the amount of starting material, and transcribed to cDNA with random hexamers using the SuperScript III First-Strand Synthesis System (Life Technologies). For quantitative PCR, reactions were performed with Brilliant II SYBR Master Mixes (Agilent Technologies), and products were analyzed with an Mx3000P QPCR System (Agilent Technologies). Primers used for RT-qPCR are provided in Supplemental Table 3. Data represent the mean ± SD of two independent experiments, each performed in duplicate. P-values were calculated using 1-way ANOVA followed by Tukey's post hoc test; * $p<0.05$, ** $p<0.001$, and *** $p<0.0001$.

Purification of GST fused Rab proteins, and Numb interaction studies

cDNAs of mouse Rab5a, 7a, 7b, and 11a were subcloned into the pGEX vector. BL21 competent E. Coli cells were transformed with expression vectors of GST-tagged Rab 5a, 7a, 7b, or 11a. After induction with 1mM isopropyl β-D-1-thiogalactopyranoside (IPTG) for four hours, bacterial proteins were extracted, and subjected to GST pull down with Glutathione Sepharose 4B (GE Healthcare Life Sciences). An aliquot of purified recombinant proteins was separated by SDS-PAGE, and purity was determined by Coomassie blue staining. To generate γGTP or GDP bound forms, GDP or GTP of purified GST-tagged Rab5a, 7a, 7b, and 11a recombinant proteins were chelated with 1mM EDTA, and subsequently GDP or GTPγS was rebound to generate inactive or active forms (11). Meanwhile, 293T cells were transiently transfected with the vector expressing Flag-tagged Numb. Cell lysates were mixed with GDP or GTPγS bound Rab 5a, 7a, 7b, or 11a recombinant proteins. After overnight

incubation, each mixture was subjected to GST-pull down, separated by SDS-PAGE, and analyzed with anti-Flag antibody.

Mouse tissue extraction and Western blotting

Embryonic heart ventricles were lysed with 1% Triton, PBS. After centrifugation, supernatants were subjected to immunoprecipitation with anti-ErbB2 monoclonal antibody (3B5, Abcam), followed by Western blotting, or directly subjected to Western blotting without immunoprecipitation. Primary antibodies used were anti-Phosphotyrosine monoclonal (4G10, Millipore, 1:400), anti-Ubiquitin monoclonal (P4D1, Cell Signaling, 1:400), anti-ErbB2 polyclonal (sc284, Santa-Cruz; 1:100), anti-pYap1 (Ser112) polyclonal (#4911, Cell signaling, 1:500), anti-Yap1 monoclonal (2F12, Abnova, 1:500), anti-pAkt monoclonal (D9E, Cell Signaling, 1:1000), anti-Akt (pan) monoclonal (C67E7, Cell Signaling, 1:500), anti-pERK1/2 monoclonal (D13.14.4E, Cell Signaling, 1:500), anti-ERK1/2 polyclonal (#9102, Cell Signaling, 1:500), anti-pFAK polyclonal (44-624G, Life Technologies, 1:400), anti-pStat3 monoclonal (D3A7, Cell Singaling, 1:400), anti-Stat3 polyclonal (#9132, Cell Signaling, 1:400), anti-pStat5 monoclonal (D47E7, Cell Signaling, 1:400), anti-Stat5 polyclonal (#9363, Cell Signaling, 1:400), anti-Cleaved Notch1 monoclonal (D3B8, Cell Signaling, 1:200), anti-Notch1 monoclonal (EP1238Y, Abcam, 1:500), anti-Numb monoclonal (C29G11, Cell Signaling, 1:250), anti-Lamp1 monoclonal (1D4B, DSHB, 1:200), and anti-Gapdh monoclonal (6C5, Santa-Cruz, 1:2000). HRP-conjugated anti-rabbit polyclonal (111-035-144, Jackson Immuno Research, 1:2000), anti-mouse polyclonal antibody (sc2005, Santa-Cruz, 1:500), or anti-rat polyclonal antibody (112-035-167, Jackson Immuno Research, 1:2000) was used as a secondary antibody. An anti-Cleaved Notch1 monoclonal antibody is the same antibody as the one used in the study showing Notch activation (12).

Western blots were quantitated with Image J software. All the Western blots of interest were normalized as indicated in figures, set the value of either control or cKO as 100, and calculated relative densitometry of target blots. Data represent the mean ± SD. P-values were calculated using unpaired two-tailed Student's t-test or 1-way ANOVA followed by Tukey's post hoc test; * $p<0.05$, ** $p<0.001$, and *** $p<0.0001$.

Generation of Numb/NumbL KO HeLa cell line

To minimize off-target effects, we utilized Nickase (13), designing single-guide RNAs (sgRNAs) for *Numb* or *NumbL* (Supplemental Figure 5C). sgRNAs1, 2, 3, or 4 were subcloned into pX335. sgRNAs for double nicking strategy were validated with pEGxxFP system (14). HeLa cells were cotransfected with sgRNA 1 and 2 for targeting Numb, or sgRNA 1, 2, 3, and 4 for targeting both Numb and NumbL, with an expression vector expressing the puromycin resistance gene, using Lipofectamine LTX with Plus Reagent (Life Technologies) on 6-well plates. Oligo sequences for sgRNA are shown in Supplemental Table 4. After cells were cultured in the presence of 3μg/ml of puromycin for 48 hours, cells were subjected to limiting dilution by plating on 96-well plates at a density of 0.8 cells/well. Wells containing more than two clones were excluded, and only wells containing single clones were further propagated. Each clone was screened by Western blotting with anti-Numb monoclonal (C29G11, Cell Signaling, 1:600) and anti-NumbL polyclonal (10111-1-AP, Proteintech, 1:400) antibodies. Genomic DNA was extracted from each clone which had lost expression of Numb or Numb/NumbL using a PureLink Genomic DNA Mini Kit (Life technologies). Targeted genomic regions of each clone were amplified with PCR, followed by subcloning into pBluescript, and sequence analysis. Edited genomic sequences of Nb/NbL KO HeLa cell clones are shown in Supplemental

Figure 5D. As shown in Figure 4B, we obtained three independent clones of Numb/NumbL KO HeLa cell lines, and used two independent clones (clone 8 and 18) for subsequent analyses.

Cell proliferation assays

Wild-type and KO HeLa cells were plated onto 96-well plates coated with Fibronectin (F1141, Sigma, 1:200) at a density of 2.8 x 10^4 or 4.3 x 10^4 cells/well. Cells were harvested at each day point, and subjected to CellTiter 96 aqueous cell proliferation assay (Promega), as indicated by the company protocol. Measurements were performed in quadruplicate with two independent experiments, and data represent the mean ± SD. P-values were calculated using 2-way ANOVA followed by Tukey's post hoc test; * $p<0.05$, ** $p<0.001$, and *** $p<0.0001$.

Quantitative analysis of intracellular vesicles

To quantitate Lamp1-positive vesicles in mouse tissue sections in a R26-mTmG indicator background (Supplemental Figure 4D), Z-stack series of pictures from 6 independent visual fields of three different samples were obtained for quantitation using an Olympus confocal microscope (FV1000). Regions of interest (ROI, trabecular myocytes) were delineated by membrane-EGFP, and Lamp1-positive vesicles inside ROI were quantitated with Image J software. The number of Lamp1-positive vesicles was normalized to the area of ROI. To quantitate Lamp1- or EEA1-positive vesicles in HeLa cells, samples were prepared from three independent experiments. Z-stack series of pictures from 6 independent visual fields per each sample were obtained for quantitation using Deltavision OMX microscope. After deconvolution, the number and/or mean volume of Lamp1 or EEA1 positive endosomes and Pearson correlation coefficients were quantitated with Volocity 3D image analysis software. Parameters were

set for the Volocity software to automatically detect each staining, and were set equally for each sample to avoid any bias (Figure 5B, E). Data represent the mean ± SD. P-values were calculated using unpaired two-tailed Student's t-test; * $p<0.05$, ** $p<0.001$, and *** $p<0.0001$. P values less than 0.05 were considered significant.

Supplemental References

1. Hirai M, Chen J, and Evans SM. Tissue-Specific Cell Cycle Indicator Reveals Unexpected Findings for Cardiac Myocyte Proliferation. *Circulation Research.* 2016;118(1):20-8.
2. Olav Z, Catherine S, Lilian H, Hye-Youn L, Estelle S, Ueli S, Lukas S, and Michel A. Multiple roles of mouse Numb in tuning developmental cell fates. *Curr Biol.* 2000;11(7).
3. Wilson A, Ardiet DL, Saner C, Vilain N, Beermann F, Aguet M, Macdonald HR, and Zilian O. Normal hemopoiesis and lymphopoiesis in the combined absence of numb and numblike. *J Immunol.* 2007;178(11):6746-51.
4. Zhang NL, Bai HB, David KK, Dong JX, Zheng YG, Cai J, Giovannini M, Liu PT, Anders RA, and Pan DJ. The Merlin/NF2 Tumor Suppressor Functions through the YAP Oncoprotein to Regulate Tissue Homeostasis in Mammals. *Developmental Cell.* 2010;19(1):27-38.
5. Jiao K, Kulessa H, Tompkins K, Zhou Y, Batts L, Baldwin HS, and Hogan BL. An essential role of Bmp4 in the atrioventricular septation of the mouse heart. *Genes & development.* 2003;17(19):2362-7.
6. Tallquist MD, and Soriano P. Epiblast-restricted Cre expression in MORE mice: a tool to distinguish embryonic vs. extra-embryonic gene function. *Genesis (New York, NY : 2000).* 2000;26(2):113-5.
7. Muzumdar MD, Tasic B, Miyamichi K, Li L, and Luo L. A global double-fluorescent Cre reporter mouse. *Genesis (New York, NY : 2000).* 2007;45(9).
8. Crone SA, Zhao YY, Fan L, Gu YS, Minamisawa S, Liu Y, Peterson KL, Chen J, Kahn R, Condorelli G, et al. ErbB2 is essential in the prevention of dilated cardiomyopathy. *Nat Med.* 2002;8(5):459-65.

9. Mizutani K-i, Yoon K, Dang L, Tokunaga A, and Gaiano N. Differential Notch signalling distinguishes neural stem cells from intermediate progenitors. *Nature.* 2007;449(7160):351-5.

10. Hirai M, Horiguchi M, Ohbayashi T, Kita T, Chien KR, and Nakamura T. Latent TGF-beta-binding protein 2 binds to DANCE/fibulin-5 and regulates elastic fiber assembly. *EMBO J.* 2007;26(14):3283-95.

11. Christoforidis S, and Zerial M. Purification and identification of novel Rab effectors using affinity chromatography. *Methods (San Diego, Calif).* 2000;20(4):403-10.

12. Zhao C, Guo H, Li JJ, Myint T, Pittman W, Yang L, Zhong WM, Schwartz RJ, Schwarz JJ, Singer HA, et al. Numb family proteins are essential for cardiac morphogenesis and progenitor differentiation. *Development.* 2014;141(2):281-95.

13. Ran FA, Patrick DH, Chie-Yu L, Jonathan SG, Silvana K, Alexandro ET, David AS, Azusa I, Shogo M, Yi Z, et al. Double Nicking by RNA-Guided CRISPR Cas9 for Enhanced Genome Editing Specificity. *Cell.* 2013;154(6).

14. Mashiko D, Fujihara Y, Satouh Y, Miyata H, Isotani A, and Ikawa M. Generation of mutant mice by pronuclear injection of circular plasmid expressing Cas9 and single guided RNA. *Sci Rep.* 2013;3(3355).

Supplemental Figure Legends

Supplemental Figure 1. **(A, B) Myocardial loss of Numb/NumbL protein in Nb/NbL cKOs: (A)** Fluorescence microscopy of ED 10.5 heart sections from control or Nb/NbL cKOs (utilizing TnTCre) in an R26-mTmG indicator background (7). Scale bar: 100µm. **(B)** Immunofluorescence microscopy of ED10.5 heart sections from control or Nb/NbL cKOs stained with DAPI to label nuclei, and antibodies to Numb and Troponin T to mark cardiomyocytes. Scale bar 100µm. **(C, D) Thicker trabeculae and loss of cells in IVS in Nb or Nb/NbL cKOs at ED10.5: (C)** Immunofluorescence microscopy of heart sections stained with DAPI to label nuclei, and antibody to TroponinT. Middle panels are magnified regions from red squares in top panels. Bottom panels are magnified images of IVS. Asterisks: loss of cells. Scale bars: 200µm for top panels, 20µm for middle and bottom panels, LV: left ventricle, T: trabeculae , IVS: interventricular septum. **(D)** Quantitative analysis of thickness and number of myocardial nuclei per length (Ctrl n=4 mice, Nb cKO n=3 mice, Nb/NbL cKO n=4 mice, 5 sections each). **(E, F) Thickness of trabeculae and compact layer in Nb or Nb/NbL cKOs at ED12.5: (E)** Immunofluorescence microscopy of ED12.5 heart sections from control and Nb/NbL cKOs, immunostained with antibodies to TroponinT. Scale bars: 200µm (top panel), 50µm (bottom panel). **(F)** Quantitative analysis of thickness of trabeculae and compact layer at ED12.5 in Nb or Nb/NbL cKOs (Ctrl n=3 mice; Nb cKO n=2 mice; Nb/NbL cKO n=3 mice, 5 sections each). LV: left ventricle, T: trabeculae, Cmpt: compact layer. **(G-I) Disorganized or thinner sarcomeres in Nb or Nb/NbL cKOs at ED10.5 and ED12.5: (G)** Immunofluorescence microscopy of heart sections stained with Phalloidin to visualize actin filaments, and antibodies to TnroponinT to visualize sarcomeric structure. Scale bars: 10µm. **(H)** Electron microscopy of trabeculae from control or Nb/NbL cKOs. White triangles indicate sarcomere length (top panel) and sarcomere thickness (bottom panel). Scale

bars: 0.5µm (top panel), 200nm (bottom panel). **(I)** Quantitative analysis of sarcomere length and thickness. (Ctrl n=4 mice; Nb/NbL cKO n=4 mice). Data represent the mean ± SD. P-values were calculated using 1-way ANOVA with Bonferroni and Holm's post hoc test in **(D, F)**, or unpaired two-tailed Student's t-test; * $p<0.05$, ** $p<0.001$, and *** $p<0.0001$.

Supplemental Figure 2. (A, B, C) Increased proliferation of trabeculae in Nb/NbL cKO: (A) CyclinA2 indicator BAC transgene. CyclinA2-LacZ-EGFP, in which, following TroponinT-Cre mediated excision, CyclinA2-EGFP is expressed selectively in cycling cardiomyocytes. Thus, myocyte identity can be ensured among any proliferating cells other than myocytes, including endocardial cells, fibroblasts and pericytes, rapidly proliferate after ED10.5. **(B)** Immunofluorescence microscopy of EdU labeled ED10.5, ED12.5, and ED14.5 heart sections in TnT-Cre;CyclinA2-LacZ-EGFP backgrounds. See Cyclin A2-EGFP coincided with EdU labeling in cardiomyocytes, and proliferating trabeculae indicated by white arrows. Trabeculae in controls ceased CyclinA2-EGFP expression, whereas trabeculae in Nb/NbL cKOs maintained CyclinA2-EGFP expression. Scale bars 100µm. **(C)** Quantitative analysis of CyclinA2-EGFP expression (proliferation) (Ctrl n=3 mice, Nb/NbL cKO n=3 mice for each stage, 5 sections each). The number of CyclinA2-EGFP positive myocytes was significantly increased in Nb/NbL cKOs relative to controls from ED10.5 through to ED14.5, while in the compact layer the number of CyclinA2-EGFP positive myocytes was not changed between controls and Nb/NbL cKOs. **(D) Decreased expression of cell cycle inhibitor Kip2/p57 in Nb/NbL cKO trabeculae:** Immunofluorescence microscopy of ED10.5 heart sections from Ctrl and Nb/NbL cKOs immunostained for markers of myocardium (TroponinT) or endocardium (Flk1) and Kip2/p57. Yellow triangles indicate nuclei of trabecular myocytes. **(E, F) Numb mRNA is selectively enriched in trabeculae**: Representative images of Eosin-stained ED10.5 heart section utilized for laser capture

microdissection: (upper panel) Trabecular regions outlined prior to microdissection; (middle panel) following dissection of trabeculae, with compact layer regions outlined prior to microdissection; (lower panel) section following capture of both trabecular and compact layer regions. **(F)** qRT-PCR analysis of Numb mRNA (n=2). Data represent the mean ± SD. P-values were calculated using two-tailed Student's t-test in **(C)**: * $p<0.05$, ** $p<0.001$.

Supplemental Figure 3. (A) Yap1 is localized to nuclei cell autonomously in Nb/NbL mutant cells: Immunofluorescence microscopy of an ED10.5 heart section of mosaic Nb/NbL cKO mouse with R26-mTmG indicator background. **(B) Western blot analyses of Nb/NbL cKOs at E12.5:** (Left) Western blot analysis of ED12.5 heart, (Right) Quantitative analysis (n=4 mice each genotype, n=7 for pStat5, * $p<0.05$). Control was set as 100. **(C) Lack of Notch activation in Nb/NbL cKOs:** Immunofluorescence microscopy of heart sections with transcriptional Notch indicator background (9). This indicator expresses GFP in cells where Notch signaling is activated. As expected from previous studies, GFP is expressed in endocardium, but not TnT expressing myocardium (red) in controls. Expression in Nb/NbL cKOs was also confined to endocardium. Notably, no ectopic myocardial expression was observed in Nb/NbL cKOs. Scale bar: 100μm. **(D, E) ErbB2 interacts with all Nb isoforms and NbL: (D)** Mouse Numb genomic locus, and Numb isoforms. Numb isoforms are generated by inclusion or exclusion of exon 3 and/or 9 by alternative splicing. **(E)** Immunoprecipitation and Western blot analyses of 293T cell extracts expressing tagged constructs for ErbB2 or ErbB4 and Numb/NumbL isoforms. **(F, G) Defining Numb isoforms expressed during heart development and in HeLa cells: (F)** RT-PCR analysis for Numb isoforms in heart. RT-PCR Primers for P1, P2, P3, and P4 are indicated with arrows in **(D)**, and sequences are listed in Supplemental Table 1. **(G)** Western blot analysis for Numb isoforms in HeLa cells and ED12.5 heart.

Data represent the mean ± SD. P-values were calculated using two-tailed Student's t-test in **(B)**: * $p<0.05$.

Supplemental Figure 4. (A-C) Specificity of Nb/NbL interaction with ErbB2 demonstrated by requirement for specific domains: (A) Schematic illustration of Numb and ErbB2 deletion mutants. Numb ΔC1 contains proline-rich region while Numb ΔC2 does not. **(B)** Immunoprecipitation and Western blot analyses of 293T cell extracts from cells transfected with expression constructs as indicated. **(C)** Schematic illustration of domains required for Numb/ErbB2 interaction. **(D) Lamp1 positive late endosomes are reduced in Nb/NbL cKOs**: Immunofluorescence microscopy of ED10.5 heart sections with R26-mTmG indicator. **(E) Quantitative analysis of Lamp1 protein in Nb/NbL cKOs:** Western blot analysis of ED12.5 heart and quantitative analysis, normalizing to Gapdh (n=4). Data represent the mean ± SD. P-values were calculated using two-tailed Student's t-test in **(E)**: $p<0.05$ is considered as significant.

Supplemental Figure 5. (A) Tagged ErbB2 construct stably expressed in HeLa cell line. **(B) Efficiency of siRNA knock-down in HeLa cells:** qRT-PCR analysis of gene knockdown in HeLa cells. Expression level was normalized to Gapdh. Relative mRNA levels were calculated by setting no oligo samples as approximately 100. Primer sequences are shown in Supplemental Table 3. Red asterisks indicate statistically significant off-target effect. **(C, D) Generation of Nb/NbL KO HeLa cell lines**: **(C)** Design of sgRNAs. sgRNA: single guide RNA, PAM: protospacer adjacent motif. **(D)** Targeted mutations within Numb and NumbL in HeLa KO cell lines. Red nucleotides indicate insertion, blue nucleotides indicate deletion or indel mutation. PAM: protospacer adjacent motif;

PAM*: sequence complementary to PAM. **(E) Yap1 nuclear localization in Nb/NbL KO HeLa cells is rescued by siRNA to ErbB2 and inhibition of Stat5. SiRNA to ErbB4 has no effect.** Immunofluorescence microscopy in Ctrl and Nb/NbL KO HeLa cells. siRNAs indicated at top. Stat5 inhibitor was added three hours before fixation. Scale bar: 20µm. **(F) Nb/NbL KO HeLa cells exhibit increased proliferation in confluent conditions.** Quantitation of CellTiter 96 Aqueous Cell Proliferation assays (MTS). (n=4) Data represent the mean ± SD. P-values were calculated using 1-way or 2-way ANOVA with Tukey's post hoc test in **(B, F)**; * $p<0.05$, ** $p<0.001$, and *** $p<0.0001$.

Supplemental Figure 6. (A-C) Numb/NumbL interact with Rab7: (A) Coomassie blue staining of purified GST-tagged proteins. **(B-E)** Immunoprecipitation and Western blot analyses of 293T cell extracts. **(B)** Numb/NumbL interact with Rab7. **(C)** Rab7a and 7b interact with NumbF and Proline-rich region of Numb. **(D,E) Numb interacts with Numb itself and NumbL: (D)** p65 isoform of Numb interacted with p65 isoform of Numb and NumbL. **(E)** Interactions between Numb/Numb and Numb/NumbL are mediated through NumbF and Proline-rich region of Numb.

Supplemental Figure 7. Summary of isoform and domain specific interactions of Numb. (A) Interactions of Numb Isoforms and NumbL with protein partners identified in this study. + or - indicates the presence or absence of interaction with proteins shown at the top. **(B)** Domains within Numb required for interaction with protein partners identified in this study.

Supplemental Tables

Supplemental Table S1. Primer sequences for RT-PCR

mouse Numb RT-P1	ATGCCGTAAAGAGATTGAAAGC
mouse Numb RT-P2	CTGTCAAAGTTCCTATCTGGGG
mouse Numb RT-P3	CCACTATGCAGAGGAAGACCGA
mouse Numb RT-P4	ACACTTCTTCTAACCAGCGGTC

Supplemental Table S2. Oligo sequences of siRNAs

Numb Silencer Select-sense	CUAAGGACCUCAUAGUUGAtt
Numb Silencer Select-antisense	UCAACUAUGAGGUCCUUAGtt
NumbL Silencer Select-sense	GGUACUUUUCUAUCUUUUAtt
NumbL Silencer Select-antisense	UAAAAGAUAGAAAAGUACCcg
ErbB2 Silencer Select-sense	GGAUCGAUAUGCCUUGGCAtt
ErbB2 Silencer Select-antisense	UGCCAAGGCAUAUCGAUCCtc
ErbB4 Silencer-sense	GUUGGAUGAUUGACUCUGAtt
ErbB4 Silencer-antisense	UCAGAGUCAAUCAUCCAACat

Supplemental Table S3. Primer sequences for qRT-PCR

mouse Numb RT-sense	AACAAACTACGGCAAAGCTTCA
mouse Numb RT-antisense	TTCTACGTGGCCGAGGTACT
mouse Gapdh RT-sense	AGGTCGGTGTGAACGGATTTG
mouse Gapdh RT-antisense	TGTAGACCATGTAGTTGAGGTCA
human Numb RT-sense	TCAGCAGATGGACTCAGAGTT
human Numb RT-antisense	AGGCTCTATCAAAGTTCCTGTCT
human NumbL RT-sense	TGGTGGACGACAAAACCAAGG
human NumbL RT-antisense	ACGACAGATATAGGAGAAAGCCT
human ErbB2 RT-sense	TGTGACTGCCTGTCCCTACAA
human ErbB2 RT-antisense	CCAGACCATAGCACACTCGG
human ErbB4 RT-sense	GCAGATGCTACGGACCTTACG
human ErbB4 RT-antisense	GACACTGAGTAACACATGCTCC
human Gapdh RT-sense	AGGTGAAGGTCGGAGTCAACG
human Gapdh RT-antisense	GATGACAAGCTTCCCGTTCTCAG

Supplemental Table S4. Oligo sequences of sgRNAs

Numb gRNA1-fwd	caccgCTGCCACTGATGTGGACGAC
Numb gRNA1-rev	aaacGTCGTCCACATCAGTGGCAGc
Numb gRNA2-fwd	caccGATGAAGAAGGCGTTCGCAC
Numb gRNA2-rev	aaacGTGCGAACGCCTTCTTCATC
NumbL gRNA3-fwd	caccgTTCACACACGTGCATTCCCC
NumbL gRNA3-rev	aaacGGGGAATGCACGTGTGTGAAc
NumbL gRNA4-fwd	caccgAGATGCGGTGAAGAAGCTGA
NumbL gRNA4-rev	aaacTCAGCTTCTTCACCGCATCTc

Supplemental Figure 1

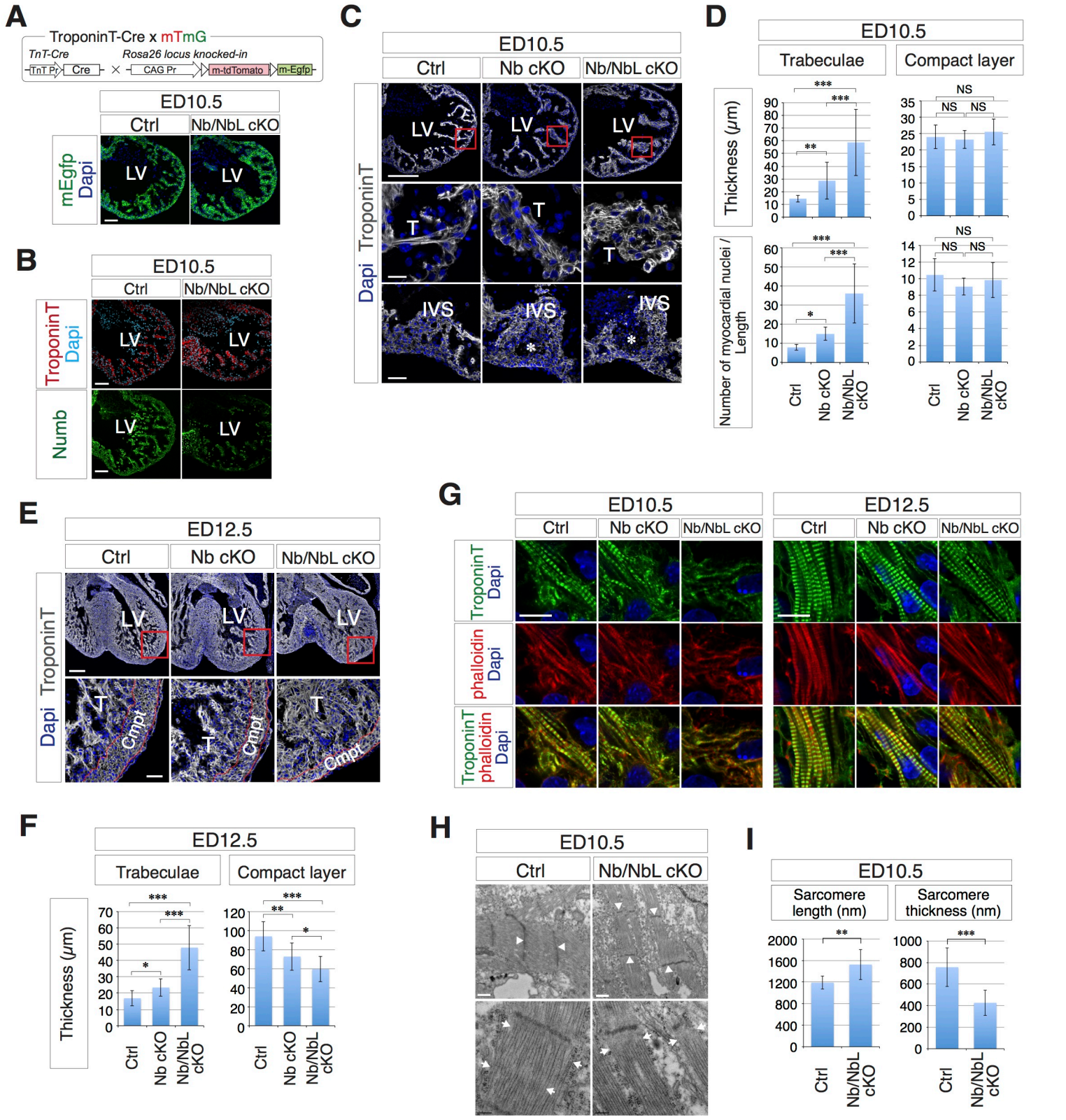

Supplemental Figure 1. (A, B) Myocardial loss of Numb/NumbL protein in Nb/NbL cKOs: (A) Fluorescence microscopy of heart sections with R26-mTmG indicator. **(B)** Immunofluorescence microscopy of heart sections. **(C, D) Thicker trabeculae and loss of cells in IVS in Nb or Nb/NbL cKOs at ED10.5: (C)** Immunofluorescence microscopy of heart sections. Middle panels are magnified regions from red squares in top panels. Asterisks: loss of cells, LV: left ventricle, T: trabeculae , IVS: interventricular septum. **(D)** Quantitative analysis of (C) (Ctrl n=4 mice, Nb cKO n=3 mice, Nb/NbL cKO n=4 mice, 5 sections each). **(E, F) Thickness of trabeculae and compact layer in Nb or Nb/NbL cKOs at ED12.5: (E)** Immunofluorescence microscopy of heart sections. **(F)** Quantitative analysis of (E) (Ctrl n=3 mice; Nb cKO n=2 mice; Nb/NbL cKO n=3 mice, 5 sections each). Cmpt: compact layer. **(G-I) Disorganized or thinner sarcomeres in Nb or Nb/NbL cKOs at ED10.5 and ED12.5: (G)** Immunofluorescence microscopy of heart sections. **(H)** Electron microscopy of trabeculae. White triangles indicate sarcomere length (top panel) and sarcomere thickness (bottom panel). **(I)** Quantitative analysis of (H) (Ctrl n=4 mice; Nb/NbL cKO n=4 mice). Data represent the mean ± SD. P-values were calculated using 1-way ANOVA with Bonferroni and Holm's post hoc test in (D, F), or unpaired two-tailed Student's t-test; * p<0.05, ** p<0.001, and *** p<0.0001.

Supplemental Figure 2

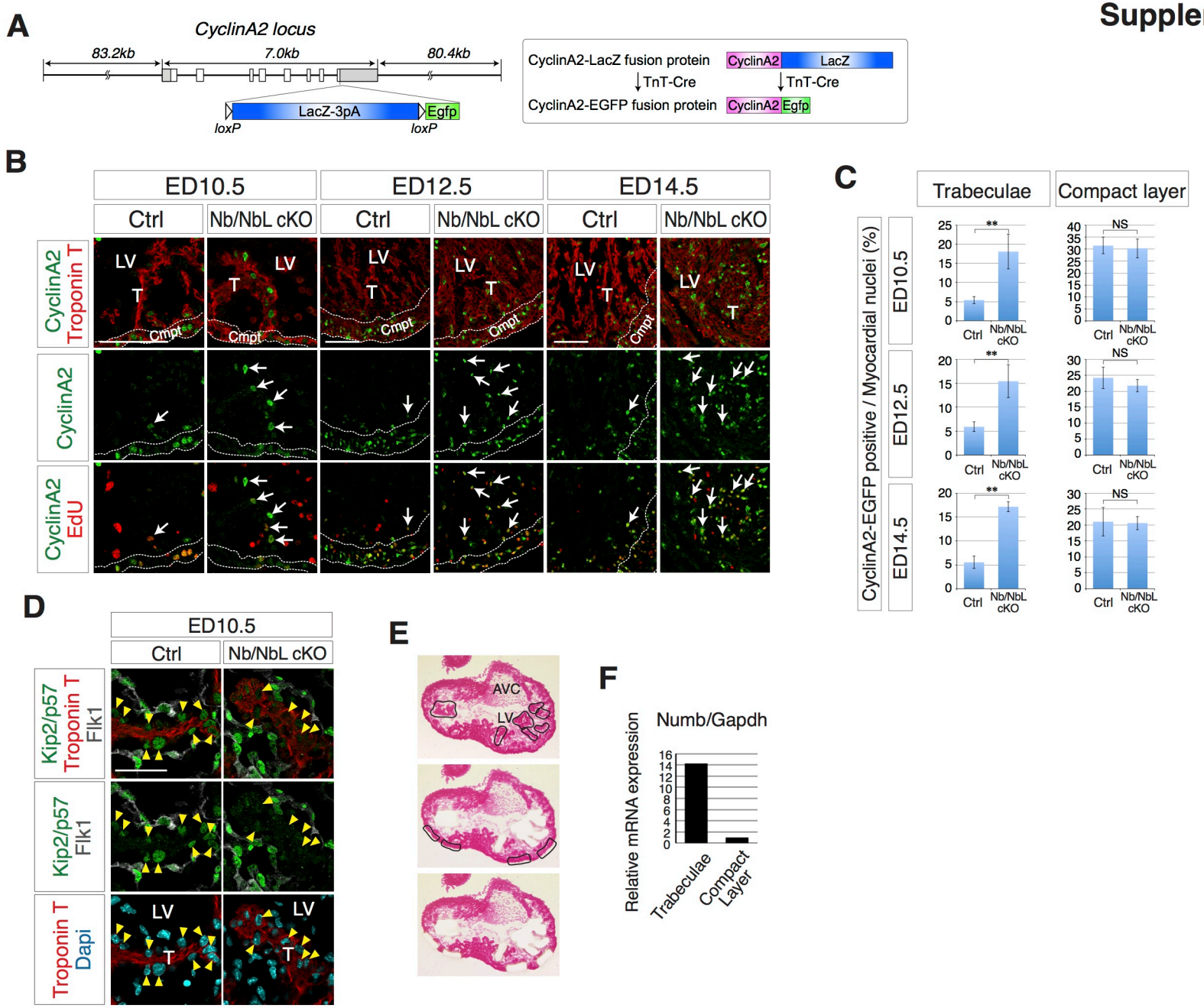

Supplemental Figure 2. (A, B, C) Increased proliferation of trabeculae in Nb/NbL cKO: (A) CyclinA2 indicator BAC transgene. CyclinA2-LacZ-EGFP, in which, following TroponinT-Cre mediated excision, CyclinA2-EGFP is expressed selectively in cycling cardiomyocytes. **(B)** Immunofluorescence microscopy of EdU labeled heart sections in TnT-Cre;CyclinA2-LacZ-EGFP backgrounds. See Cyclin A2-EGFP coincided with EdU labeling in cardiomyocytes, indicated by white arrows. Trabeculae in controls ceased CyclinA2-EGFP expression, whereas trabeculae in Nb/NbL cKOs maintained CyclinA2-EGFP expression. **(C)** Quantitative analysis of CyclinA2-EGFP expression (proliferation) (Ctrl n=3 mice, Nb/NbL cKO n=3 mice for each stage, 5 sections each). **(D) Decreased expression of cell cycle inhibitor Kip2/p57 in Nb/NbL cKO trabeculae:** Immunofluorescence microscopy of heart sections. Yellow triangles indicate nuclei of trabecular myocytes. **(E, F) Numb mRNA is selectively enriched in trabeculae: (E)** Representative images of ED10.5 heart section utilized for laser capture microdissection. **(F)** qRT-PCR of Numb mRNA (n=2 each). Data represent the mean ± SD. P-values were calculated using two-tailed Student's t-test in (C): * $p<0.05$, ** $p<0.001$.

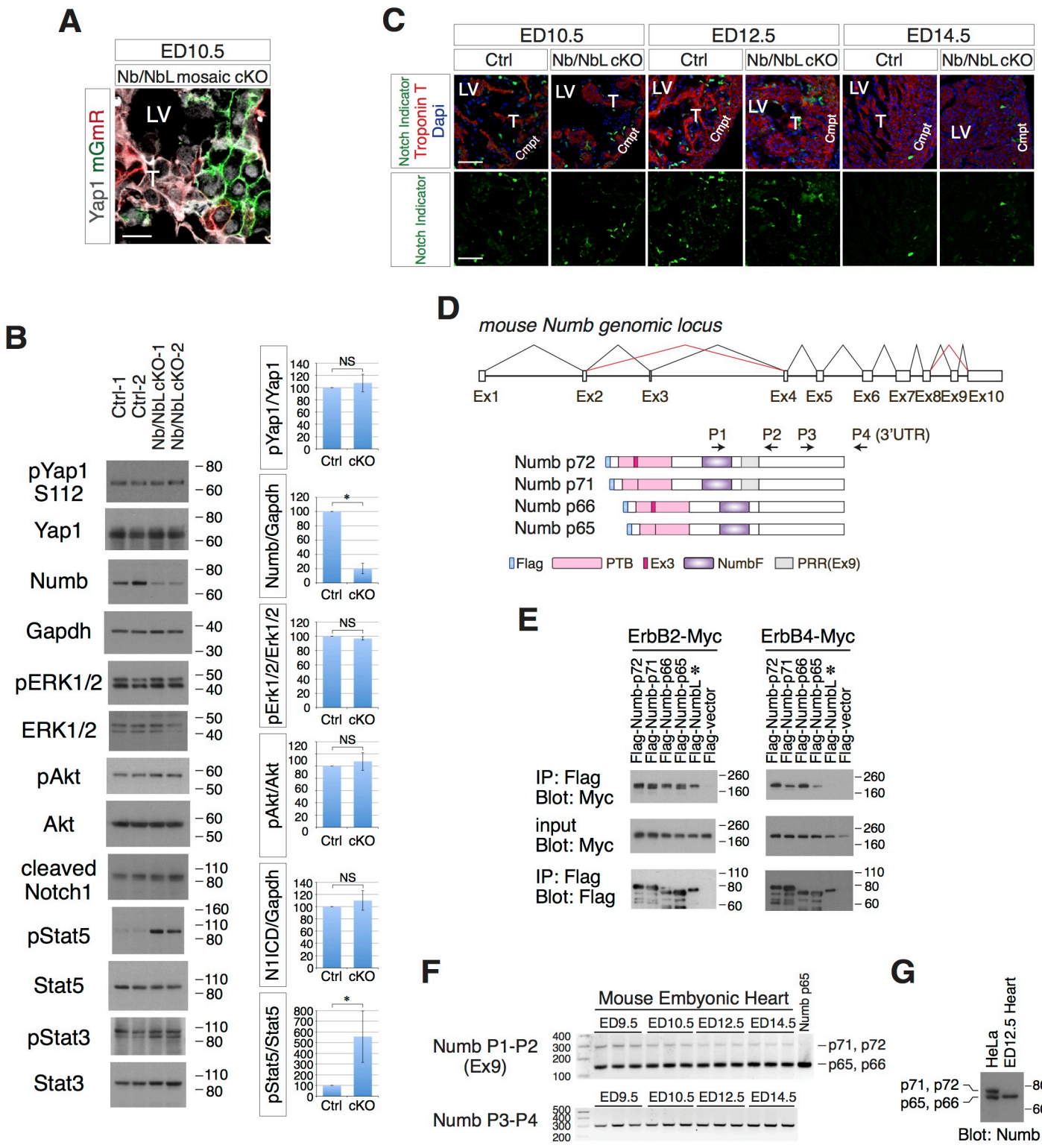

Supplemental Figure 3. (A) Yap1 is localized to nuclei cell autonomously in Nb/NbL mutant cells: Immunofluorescence microscopy of a heart section of mosaic Nb/NbL cKO mouse with R26-mTmG indicator background. **(B) Western blot analyses of Nb/NbL cKOs at E12.5:** (Left) Western blot analysis of ED12.5 heart, (Right) Quantitative analysis (n=4 mice each genotype, n=7 for pStat5, * $p<0.05$). Control was set as 100. **(C) Lack of Notch activation in Nb/NbL cKOs:** Immunofluorescence microscopy of heart sections with transcriptional Notch indicator background (Mizutani et al., 2007). This indicator expresses GFP in cells where Notch signaling is activated. **(D, E) ErbB2 interacts with all Nb isoforms and NbL: (D)** Mouse Numb genomic locus, and Numb isoforms. Numb isoforms are generated by inclusion or exclusion of exon 3 and/or 9 by alternative splicing. **(E)** Immunoprecipitation and Western blot analyses of 293T cell extracts. **(F, G) Defining Numb isoforms expressed during heart development and in HeLa cells: (F)** RT-PCR analysis for Numb isoforms in heart. RT-PCR Primers for P1, P2, P3, and P4 are indicated with arrows in (D). **(G)** Western blot analysis for Numb isoforms. Data represent the mean ± SD. P-values were calculated using two-tailed Student's t-test in (B): * $p<0.05$.

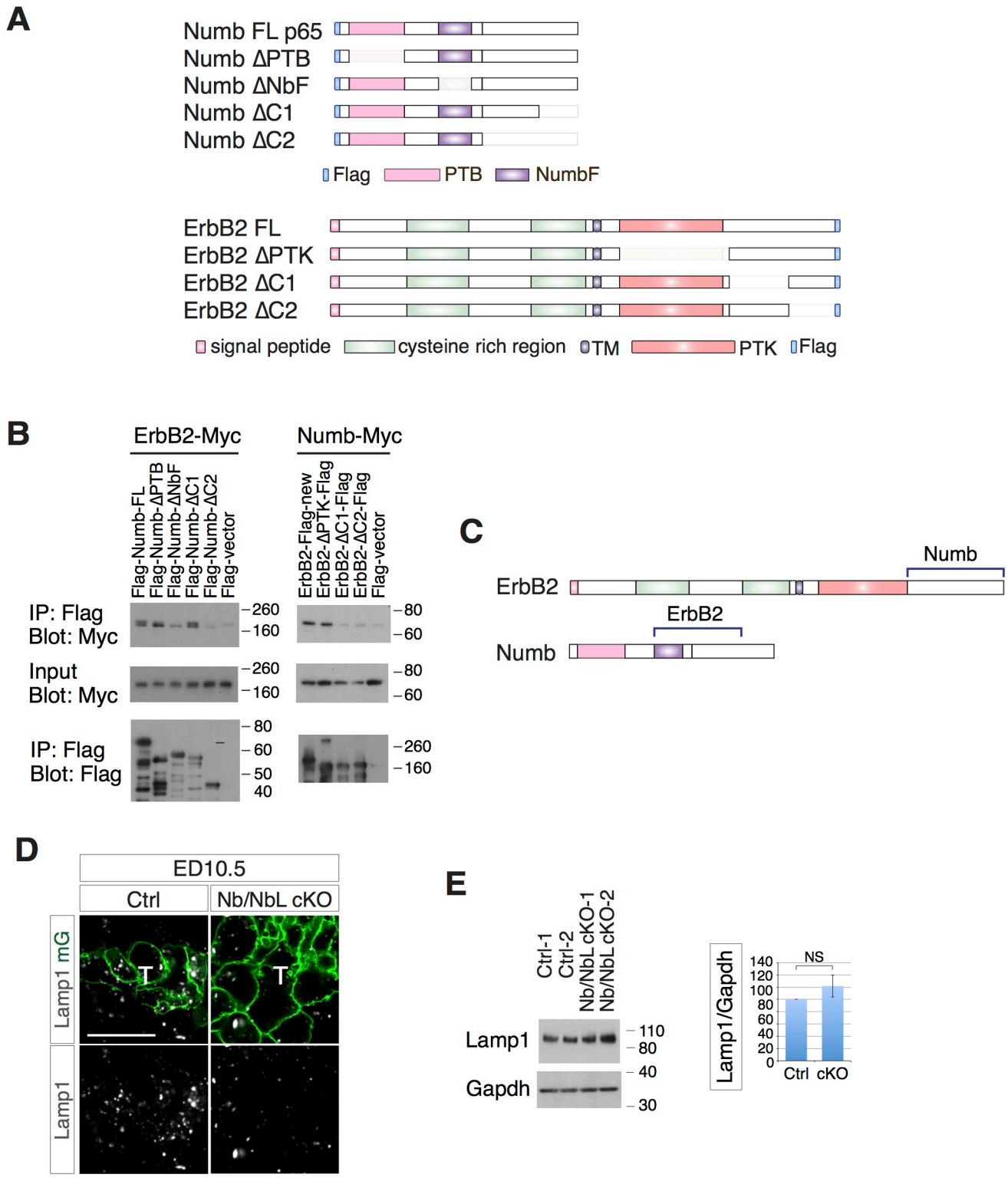

Supplemental Figure 4. (A-C) Specificity of Nb/NbL interaction with ErbB2 demonstrated by requirement for specific domains: **(A)** Schematic illustration of Numb and ErbB2 deletion mutants. Numb ΔC1 contains proline-rich region while Numb ΔC2 does not. **(B)** Immunoprecipitation and Western blot analyses of 293T cell extracts from cells transfected with expression constructs as indicated. **(C)** Schematic illustration of domains required for Numb/ErbB2 interaction. **(D) Lamp1 positive late endosomes are reduced in Nb/NbL cKOs**: Immunofluorescence microscopy of ED10.5 heart sections with R26-mTmG indicator. **(E) Quantitative analysis of Lamp1 protein in Nb/NbL cKOs**: Western blot analysis of ED12.5 heart and quantitative analysis, normalizing to Gapdh (n=4). Data represent the mean ± SD. P-values were calculated using two-tailed Student's t-test in **(E)**: $p<0.05$ is considered as significant.

Supplemental Figure 5

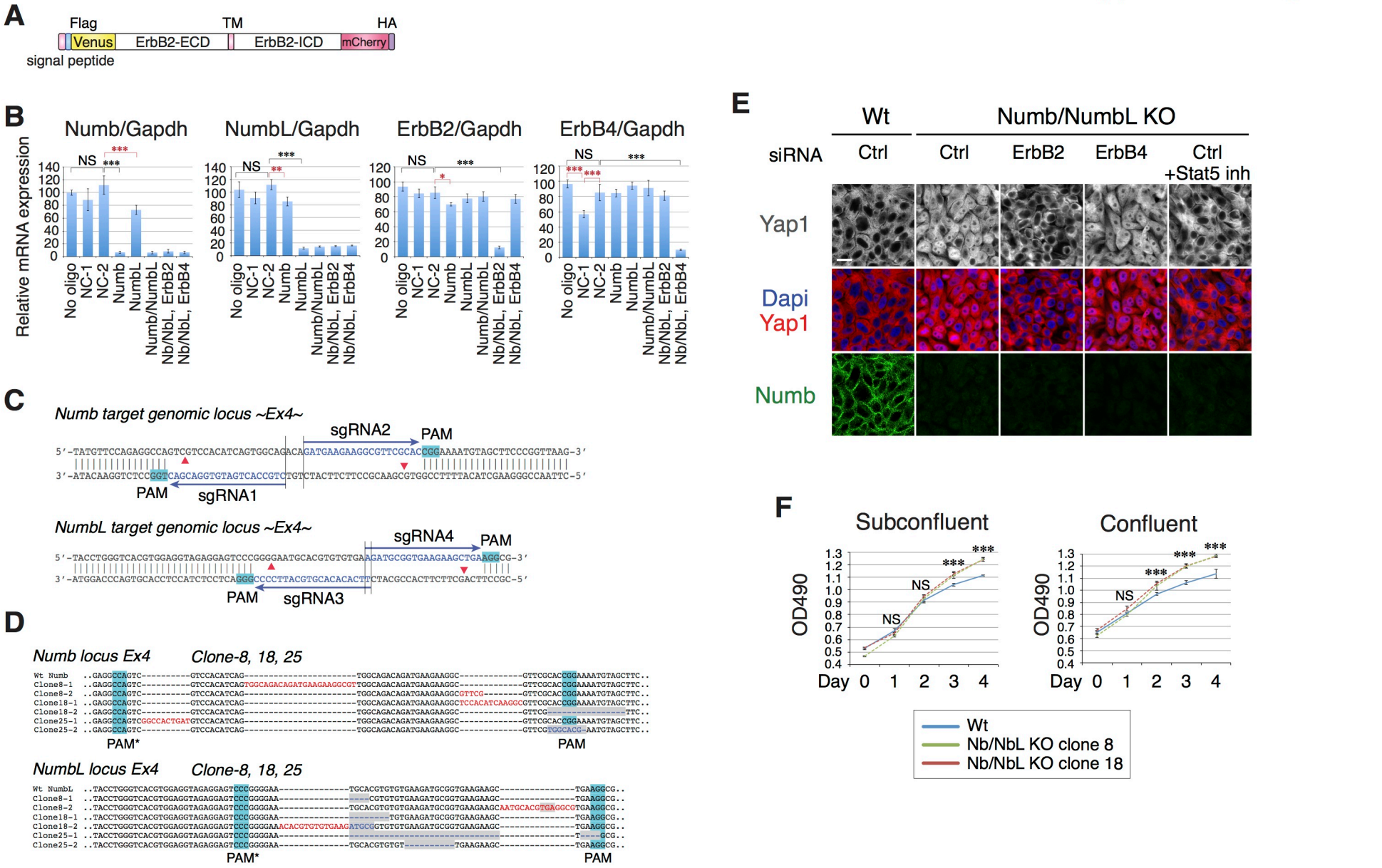

Supplemental Figure 5. (A) Tagged ErbB2 construct stably expressed in HeLa cell line. (B) Efficiency of siRNA knock-down in HeLa cells: qRT-PCR analysis of gene knockdown in HeLa cells. Expression level was normalized to Gapdh. Relative mRNA levels were calculated by setting no oligo samples as approximately 100. Primer sequences are shown in Supplemental Table 3. Red asterisks indicate statistically significant off-target effect. **(C, D) Generation of Nb/NbL KO HeLa cell lines: (C)** Design of sgRNAs. sgRNA: single guide RNA, PAM: protospacer adjacent motif. **(D)** Targeted mutations within Numb and NumbL in HeLa KO cell lines. Red nucleotides indicate insertion, blue nucleotides indicate deletion or indel mutation. PAM: protospacer adjacent motif; PAM*: sequence complementary to PAM. **(E) Yap1 nuclear localization in Nb/NbL KO HeLa cells is rescued by siRNA to ErbB2 and inhibition of Stat5. SiRNA to ErbB4 has no effect.** Immunofluorescence microscopy in Ctrl and Nb/NbL KO HeLa cells. siRNAs indicated at top. Stat5 inhibitor was added three hours before fixation. Scale bar: 20μm. **(F) Nb/NbL KO HeLa cells exhibit increased proliferation in confluent conditions.** Quantitation of CellTiter 96 Aqueous Cell Proliferation assays (MTS). (n=4) Data represent the mean ± SD. P-values were calculated using 1-way or 2-way ANOVA with Tukey's post hoc test in (B, F); * p<0.05, ** p<0.001, and *** p<0.0001.

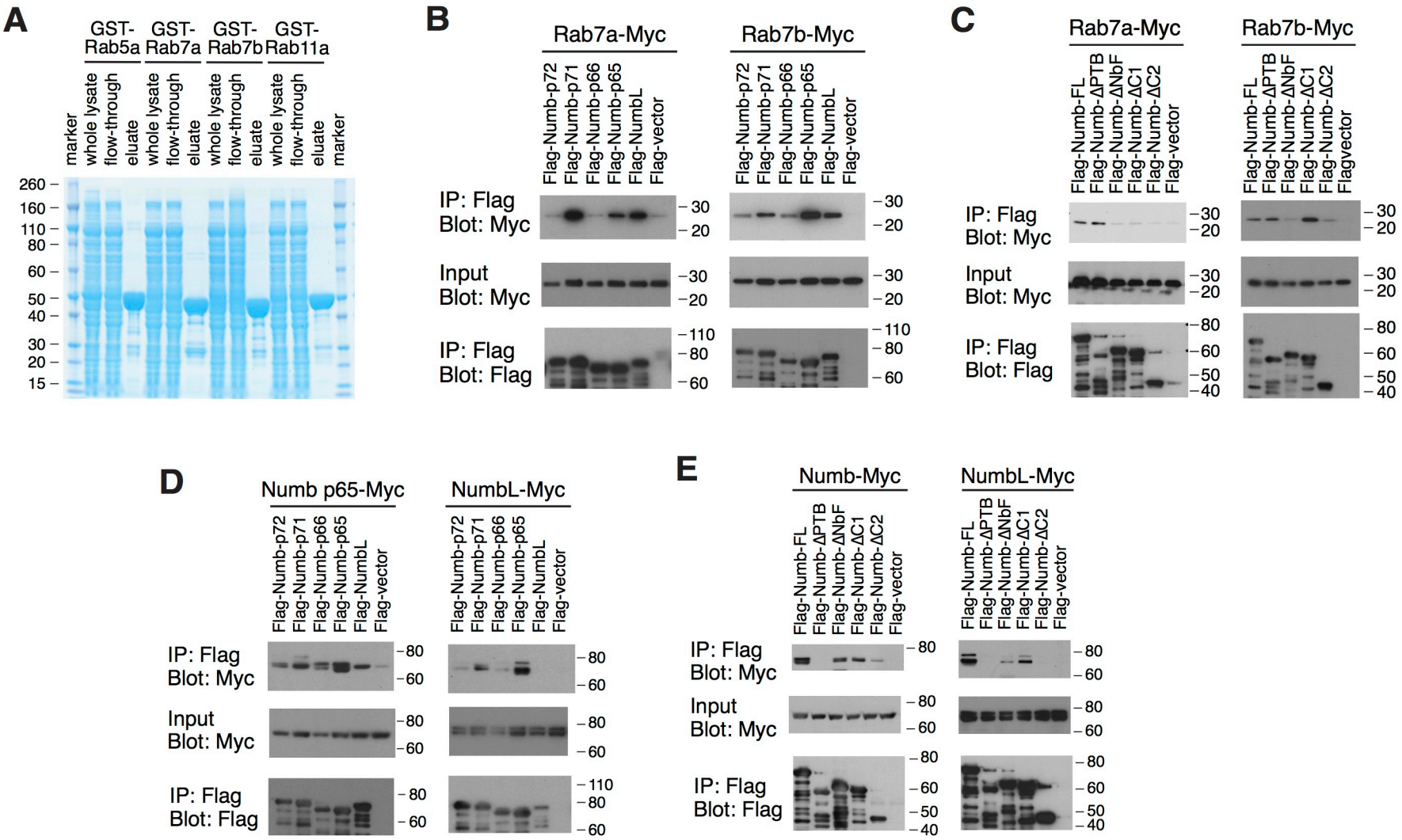

Supplemental Figure 6. (A-C) Numb/NumbL interact with Rab7: **(A)** Coomassie blue staining of purified GST-tagged proteins. **(B-E)** Immunoprecipitation and Western blot analyses of 293T cell extracts. **(B)** Numb/NumbL interact with Rab7. **(C)** Rab7a and 7b interact with NumbF and Proline-rich region of Numb. **(D,E) Numb interacts with Numb itself and NumbL: (D)** p65 isoform of Numb interacted with p65 isoform of Numb and NumbL. **(E)** Interactions between Numb/Numb and Numb/NumbL are mediated through NumbF and Proline-rich region of Numb.

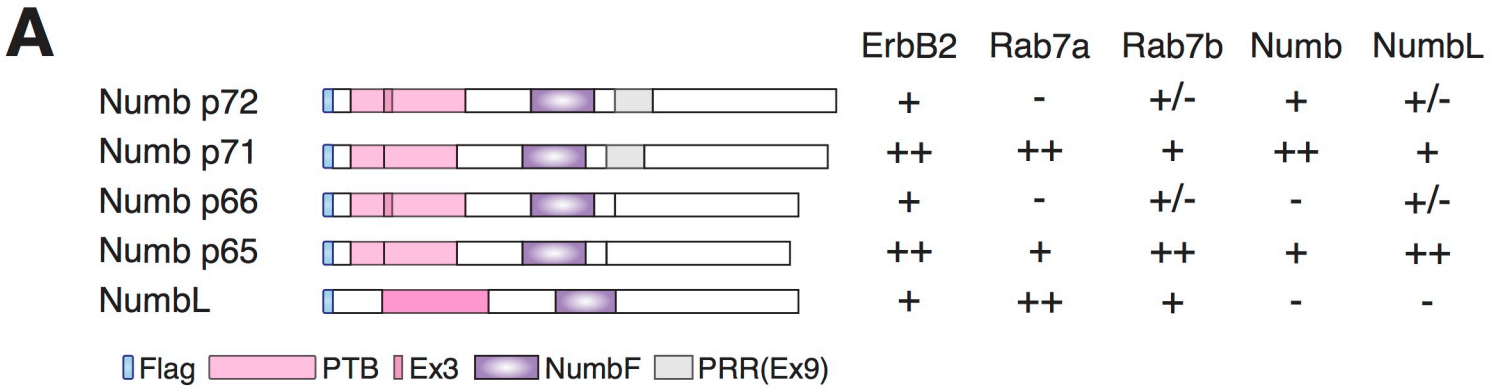

Supplemental Figure 7. Summary of isoform and domain specific interactions of Numb. (A) Interactions of Numb Isoforms and NumbL with protein partners identified in this study. + or - indicates the presence or absence of interaction with proteins shown at the top. **(B)** Domains within Numb required for interaction with protein partners identified in this study.

Full unedited gels for Figure 2 and Figure 3

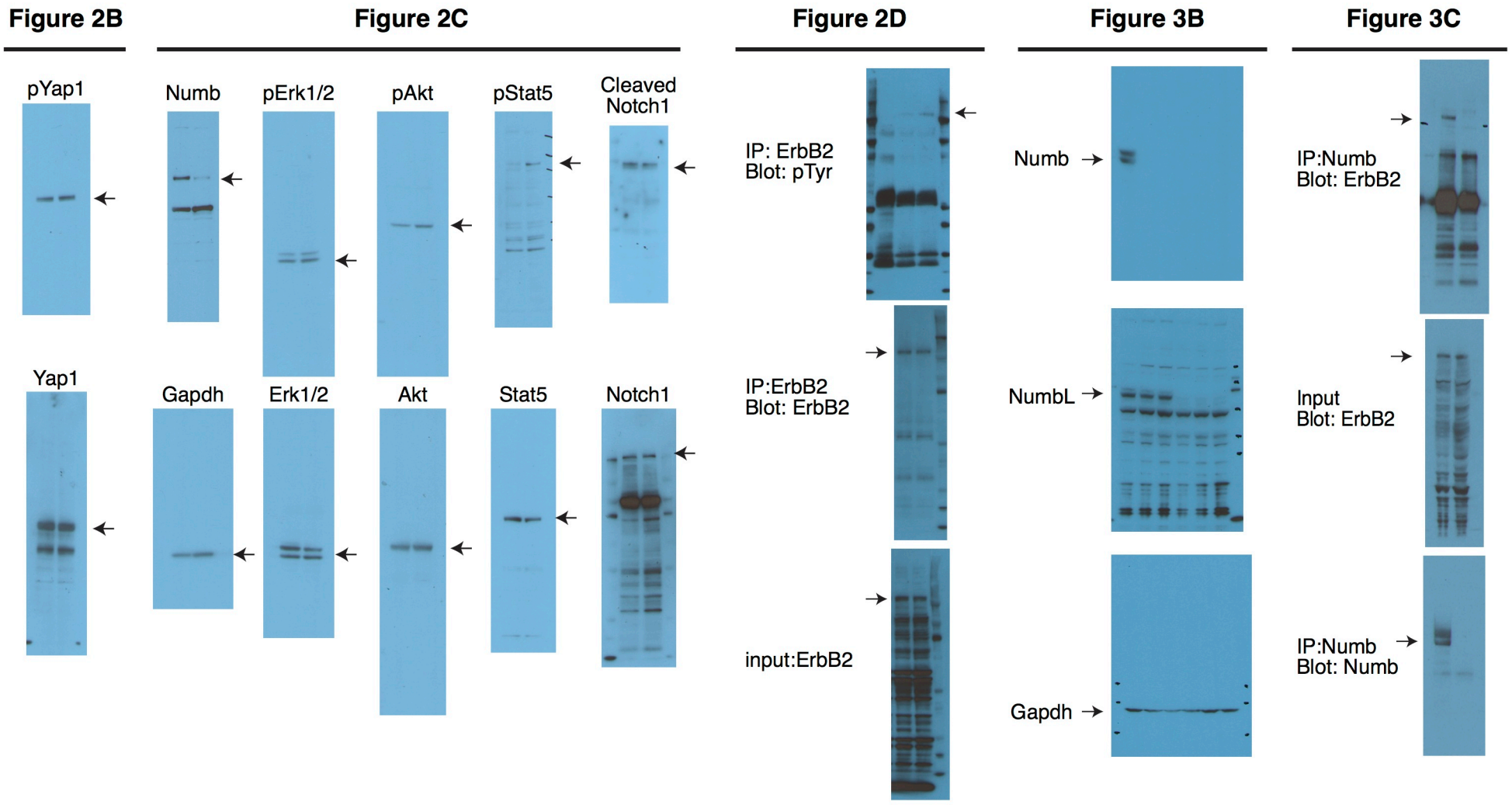

Full unedited gels for Figure 4 and Figure5

Figure 4A

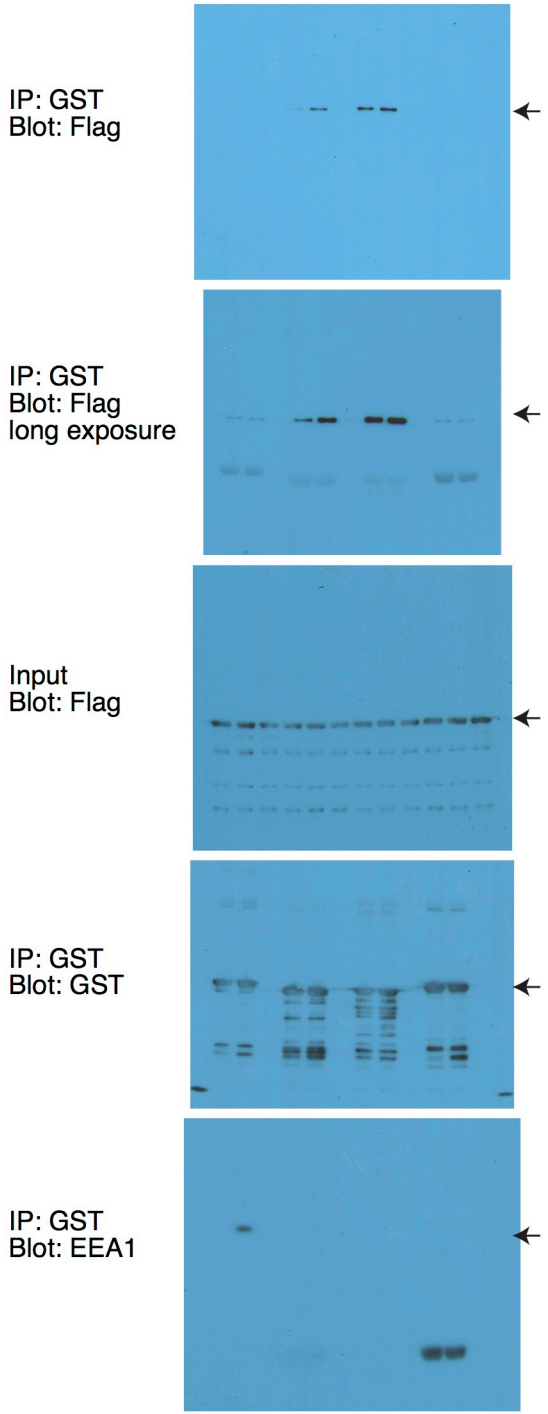

Figure 4D

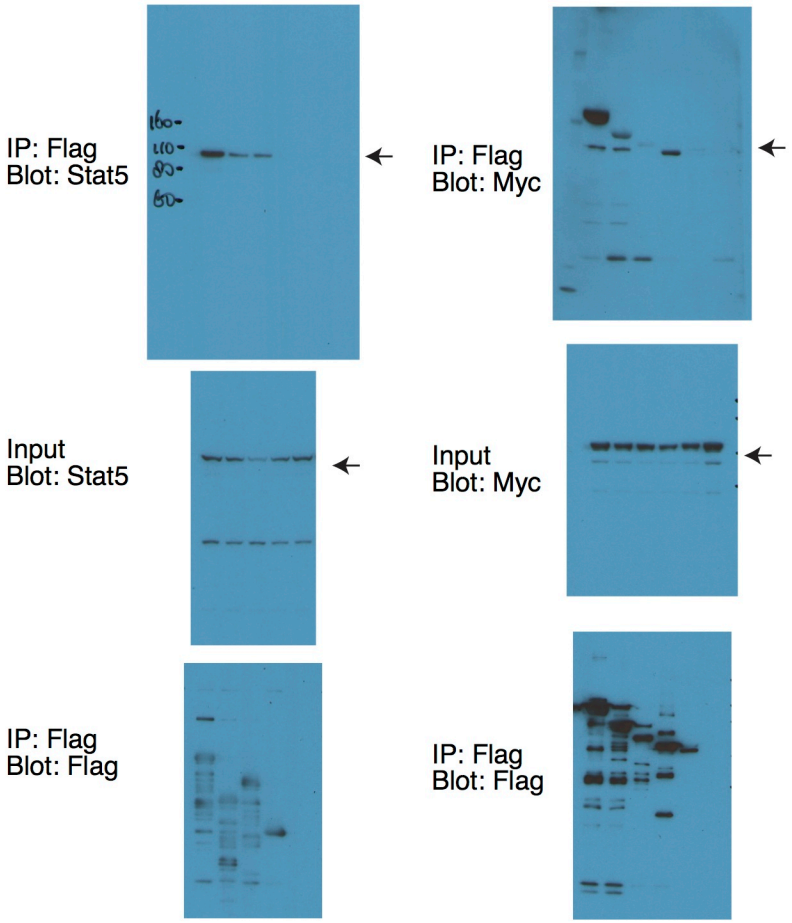

Figure 5E

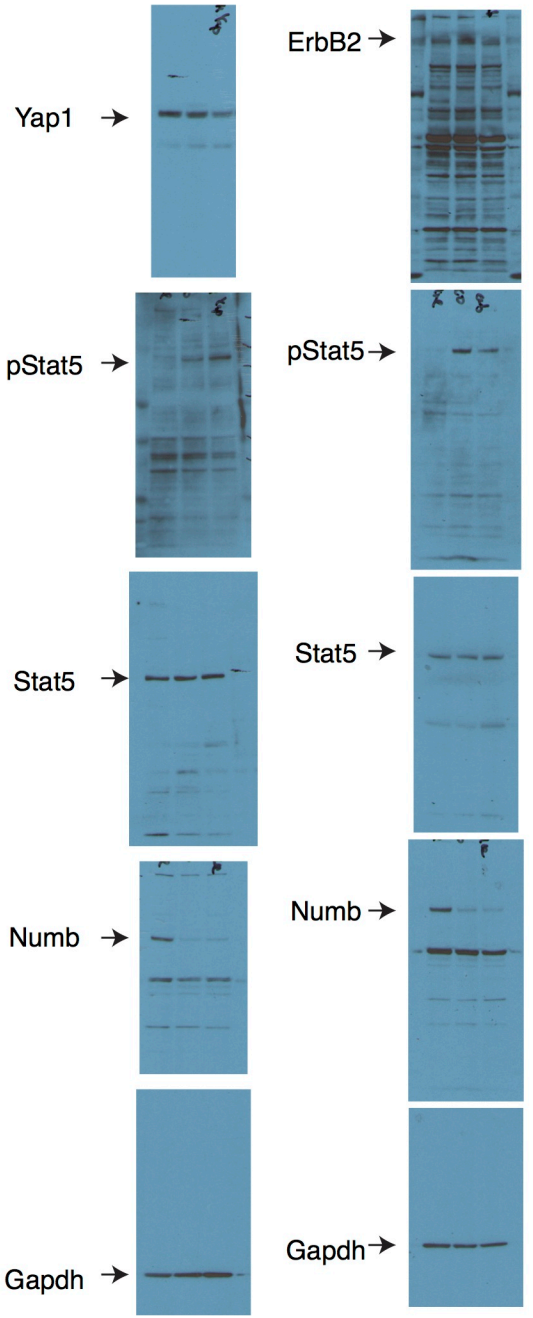

Full unedited gels for Supplemental Figure 3

Supplemental Figure 3B

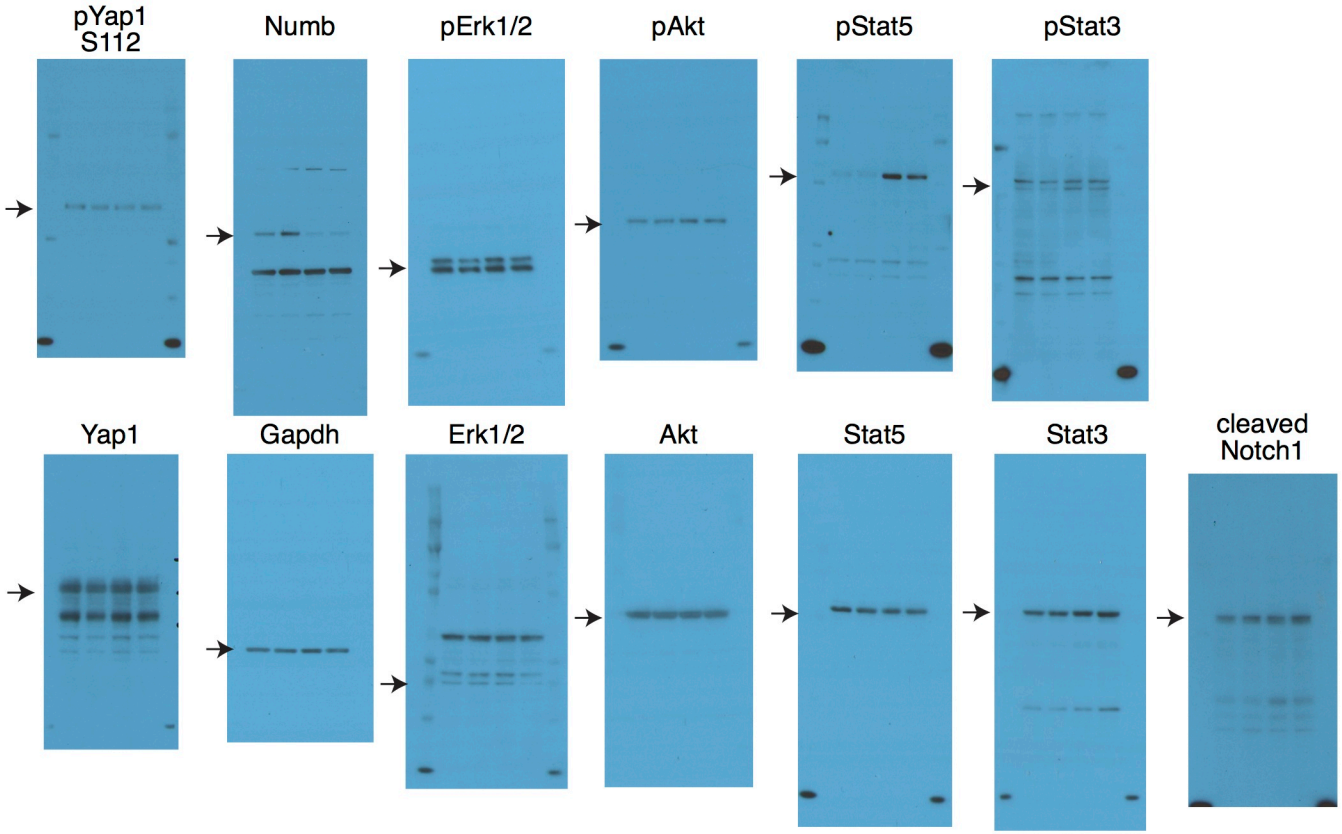

Supplemental Figure 3E

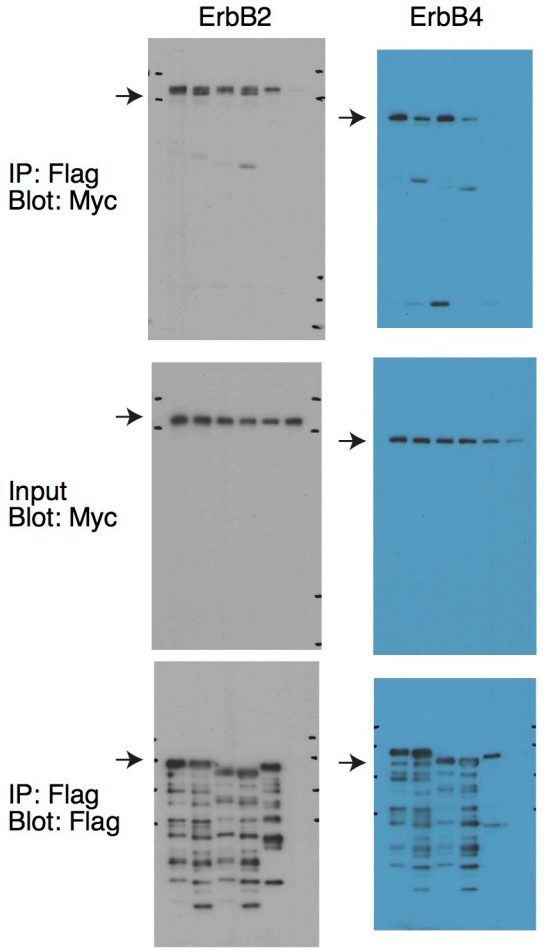

Supplemental Figure 3F

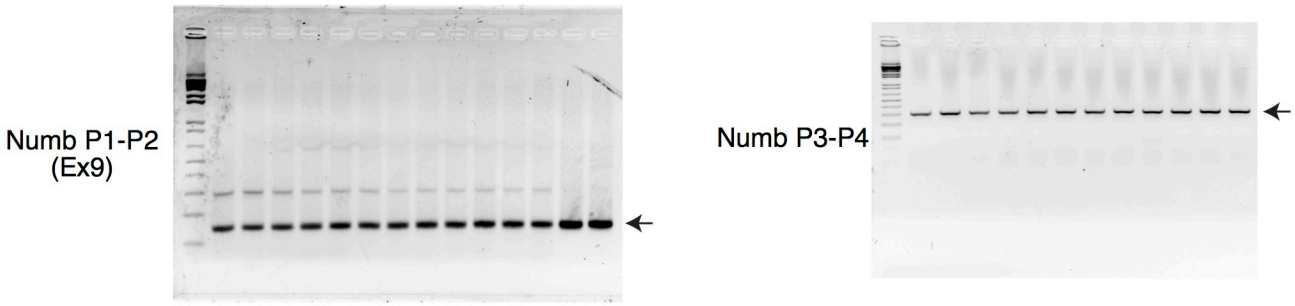

Supplemental Figure 3G

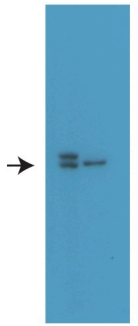

Full unedited gels for Supplemental Figure 4

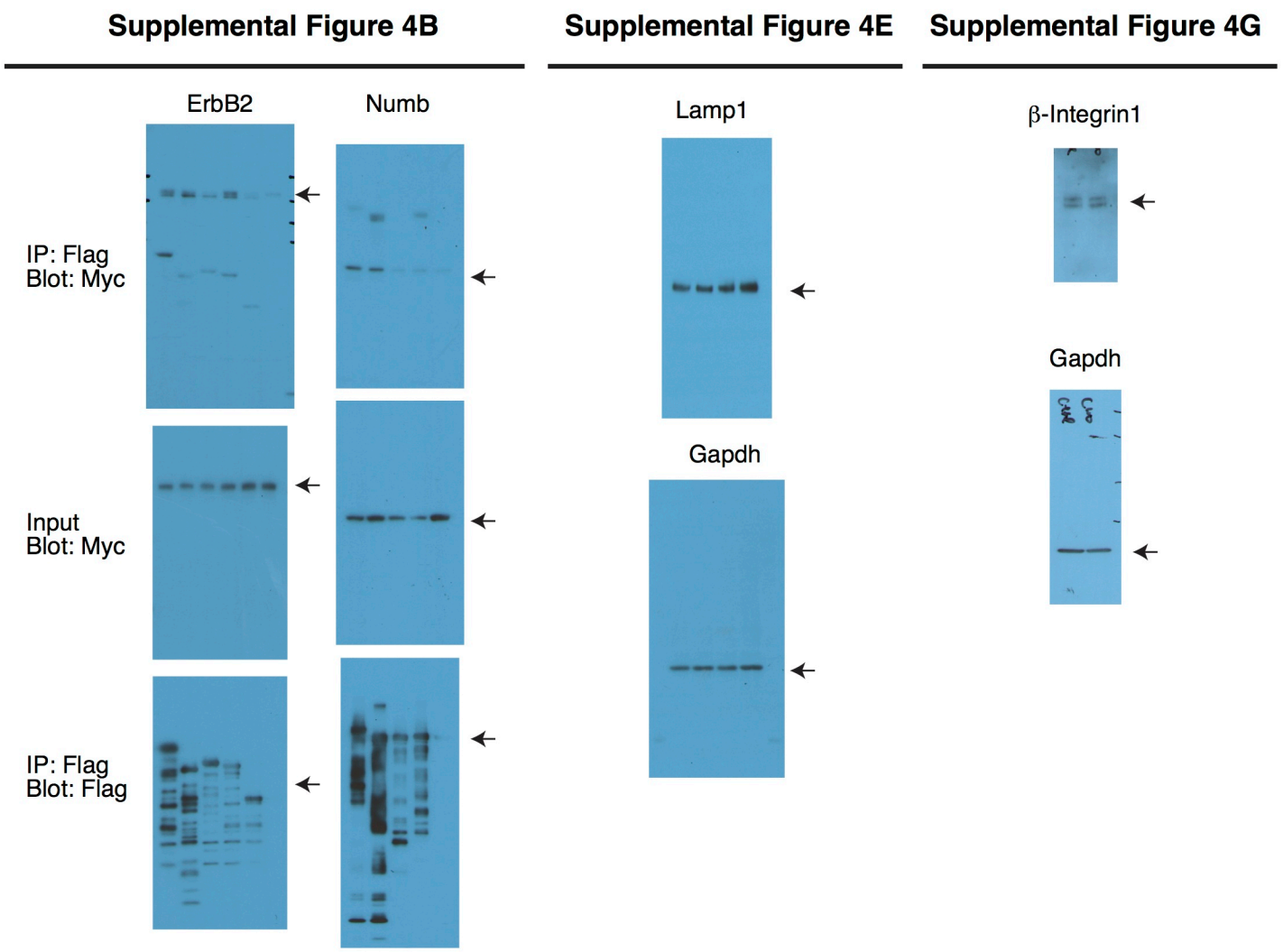

Full unedited gels for Supplemental Figure 6

Supplemental Figure 6B

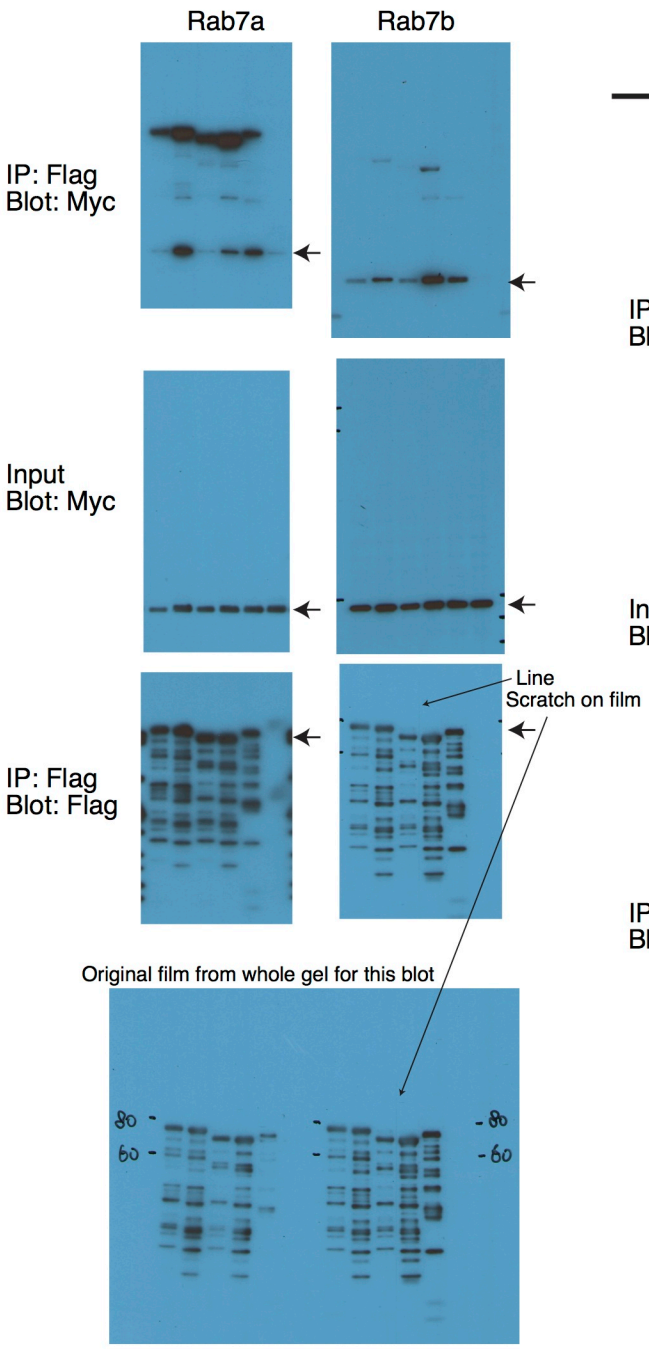

Supplemental Figure 6C

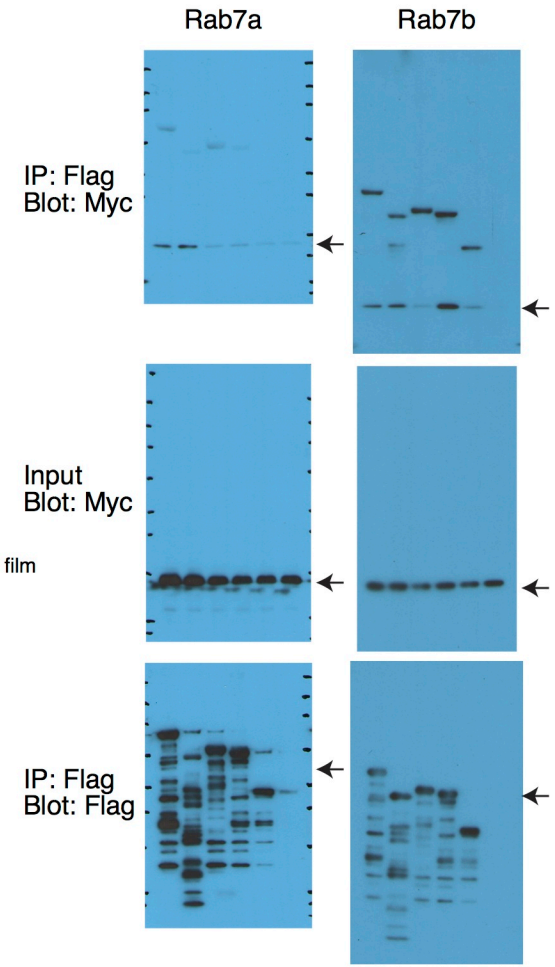

Supplemental Figure 6D

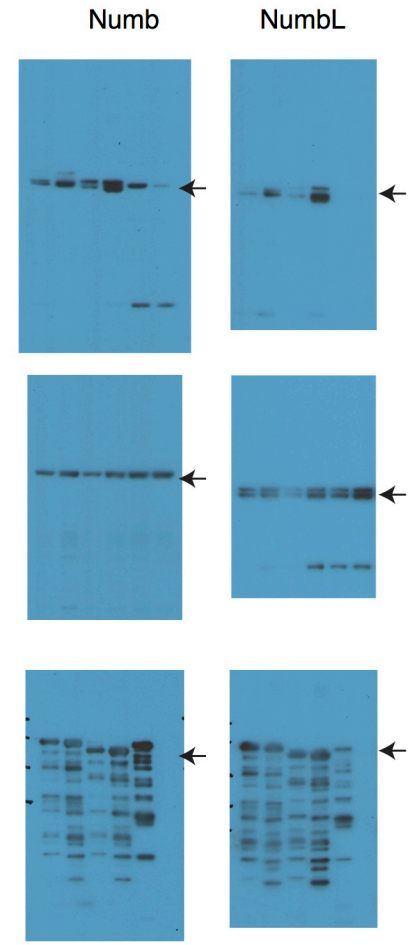

Supplemental Figure 6E